



# Lab on a Chip

## Temporal sorting of microdroplets can identify productivity differences of itaconic acid from libraries of *Yarrowia lipolytica*

Journal:	<i>Lab on a Chip</i>
Manuscript ID	LC-ART-01-2023-000020.R1
Article Type:	Paper
Date Submitted by the Author:	18-Mar-2023
Complete List of Authors:	Bowman, Emily; The University of Texas at Austin, Interdisciplinary Life Sciences Tran, Phuong Hoang Nguyen; Korea Institute of Science and Technology Gordillo Sierra, Angela; The University of Texas at Austin, Chemical Engineering Vieira Nogueira, Karoline; University of Sao Paulo Alper, Hal; The University of Texas at Austin, Chemical Engineering

SCHOLARONE™  
Manuscripts

## ARTICLE

Temporal sorting of microdroplets can identify productivity differences of itaconic acid from libraries of *Yarrowia lipolytica*Emily K. Bowman,<sup>\*a</sup> Phuong T. Nguyen Hoang<sup>b</sup>, Angela R. Gordillo Sierra<sup>c</sup>, Karoline M. Vieira Nogueira<sup>d</sup>, and Hal S. Alper<sup>a,c</sup>Received 00th January 20xx,  
Accepted 00th January 20xx

DOI: 10.1039/x0xx00000x

Microdroplet screening of microorganisms can improve the rate of strain selection and characterization within the canonical Design-Build-Test paradigm. However, a full analysis of the microdroplet environment and how well these conditions translate to culturing conditions and techniques is lacking in the field. Quantification of three different biosensor/analyte combinations at 12-hour timepoints reveal the potential for extended dose-response ranges as compared to traditional *in vitro* conditions. Using these dynamics, we present an application and analysis of microfluidic droplet screening utilizing whole-cell biosensors, ultimately identifying an altered productivity profile of itaconic acid in a *Yarrowia lipolytica*-based piggyBac transposon library. Specifically, we demonstrate that the timepoint for microdroplet selection can influence the outcome of the selection and thus shift the identified strain productivity and final titer. In this case, strains selected at earlier timepoints showed increased early productivity in flask scale, with the converse true as well. Differences in response indicate microdroplet assays require tailored development to more accurately sort for phenotypes that are scalable to larger incubation volumes. Likewise, these results further highlight that screening conditions are critical parameters for success in high-throughput applications.

## Introduction

High throughput microbial engineering relies heavily upon the canonical Design-Build-Test cycle (1, 2). While recent advances in DNA design and synthesis have helped usher in this capacity for high-throughput biology, they also create a substantial bottleneck in the test step, thus requiring more creative solutions for high throughput screening of microbial strains (3-6). Efforts to switch away from bulk liquid handling and long chromatography/separation dependent analysis techniques help improve the throughput of the test step. Certainly, established methods such as fluorescence activated cell sorting, microtiter plate cultivation, and agar-plate based screens represent alternatives. In contrast, the fluidics miniaturization and parallel culturing capability of microfluidic droplet systems help bypass many of the limitation in high-throughput metabolic engineering that are inherent even in these alternative approaches (2, 7-10). To this end, microdroplet systems uniquely enable a physical encapsulation of cells and their extracellular phenotypes such as small molecule secretion.

A remaining challenge for microdroplet screening is the capacity to transduce a chemical concentration into a rapidly detectable signal. Recent applications accomplish this task through to the use of cell based biosensors (2, 7-11), chemical sensors (12),

growth-based assays (10), and even mass spectroscopy for label-free sorting (13). However, the true utility and adoption of high throughput microdroplet screening and selection is predicated on its capability to deliver strains that perform as expected outside of the microdroplet. Limited studies have attempted to draw parallels between microdroplet and liquid phase production, especially as it relates to the parameter of time and production.

Overall assumptions regarding microdroplet sorting systems have led to difficulties in scaling identified strains (5, 14, 15). Specifically, the small-volume environments of microdroplets often identify condition-specific, beneficial gene perturbations that may not perform similarly in flask or bioreactor conditions (5). Moreover, iterative and prolonged microdroplet-based high throughput screening (as with any screen with an inherent growth step) inadvertently creates a selective environment for increased biomass—a phenotype that often negatively correlates with metabolic flux for small molecule production (16, 17). Compounded on these challenges, previous work has observed inconsistencies in strain performance upon scale-up, specifically comparing small-scale cultivation to larger scale bioreactors (17). These challenges aside, previous applications of fluorescent based microfluidic sorting have typically utilize the same incubation time used in larger cultures, including our own prior efforts (7, 9, 18). However, full characterization of the microdroplet environment is still on-going, as analysis of microdroplets is limited by access to analytical devices for immobilizing microdroplets for prolonged observation, as well as sensitive sensing and measuring techniques such as Mass Spectrometry Assisted Droplet Sorting (MADS) (13, 14).

Despite many challenges, the microdroplet environment, while clearly very different from other culturing methods including bioreactors, flasks, tubes, and even deep well plates (14, 15), is well-suited for selections and thus necessitating studies on cellular dynamics. More specifically, limited studies have investigated the importance of time-based selections when using these pico-liter sized microdroplets as a means of selecting for larger-scale

a) Interdisciplinary Life Sciences Graduate Program, The University of Texas at Austin, Austin, TX 78712; b) Korea Institute of Science and Technology (KIST), Seoul 02792, Republic of Korea; c) McKetta Department of Chemical Engineering, The University of Texas at Austin, Austin, TX 78712; d) Molecular Biotechnology Laboratory, Department of Biochemistry and Immunology, Ribeirao Preto Medical School (FMRP), University of Sao Paulo, Ribeirao Preto, SP, Brazil

† Footnotes relating to the title and/or authors should appear here.  
Electronic Supplementary Information (ESI) available: [details of any supplementary information available should be included here]. See DOI: 10.1039/x0xx00000x

productivity trends. To address these limitations, this work seeks to answer the question of whether the time-dependent selections in microdroplets will correspond to the fermentation profiles of strains outside of microdroplet conditions. Put another way, this work seeks to identify whether microdroplet selections can be used to select for shifts in cell productivity and thus achieve more exponential or more stationary phase production.

As an initial characterization, we studied the biosensor dynamics of three separate whole cell biosensors with known production strains. Once we identified a product with the greatest dynamic range in microdroplets, we investigated the influence of time-dependent selections (in this case, 24, 48, 72, and 96 hour) in microdroplets on the identification and performance of *Yarrowia lipolytica* strains for itaconic acid production using a transposon mutagenesis library. We demonstrate that sorts conducted earlier indeed result in identifying strains that show improved early productivity outside of the microdroplet. Likewise, the corollary is also proven that later-timepoint sorts identify strains better suited for production later in the culturing process. Finally, through in microdroplet characterization of production, we can demonstrate the correspondence of the pico-liter culturing environments to larger-scale cultivation techniques. Ultimately, this work identified strains that were enriched for distinct production phenotypes including increased exponential productivity (a disruption in *Ypgm1*) and higher final titer/growth independent production (a disruption in *Ygsy1*).

## Materials and Methods

### Strain Cultivation

All *Yarrowia lipolytica* production strains (2, 7, 19) were grown in either YPD containing 2% glucose (for microdroplet analysis and large flask time-course), or Yeast synthetic defined (YSD) media (2% glucose, YNB (Difco 6.7g/L), CSM complete (Thomas Scientific)). Naringenin production strains also utilize p-coumaric acid at a final concentration of 2mM as previously described (20). Flask cultures were grown at 28°C and shaken at 225rpm. Novec 7500 fluorinated oil was used due to its inherent oxygen permeability. Fresh oil was assumed to be oxygenated through atmospheric exposure as it is easily gas-permeable. Microdroplet encapsulated cultures were grown in a standing incubator at 28°C with oil-changes every 12-hour to maintain oxygenation of culture. *E. coli* itaconic acid biosensor (21) was pre-cultured before microdroplet encapsulation in LB-Kan (50ug/ml) at 37C for 18 hours. *E. coli* Naringenin and TAL biosensors were pre-cultured as previously described (7).

### Cell Encapsulation in Microdroplets

Production strains used here were those developed previously for TAL(22), Naringenin (20) and Itaconic Acid production(19). *Yarrowia lipolytica* production strains were encapsulated at a rate of 0.1 cells per microdroplet. Their corresponding biosensor cells were co-encapsulated at a rate of 10 cells per microdroplet. Encapsulation for the time courses was performed in two rounds, with timepoints taken from the same encapsulation at timepoint 0 as well as 12- and 24-hour intervals to achieve response curves.

Piggybac library generation in the itaconic acid producing strain of *Yarrowia lipolytica* took place as previously described(7). *Yarrowia lipolytica* piggyBac library members were encapsulated in microdroplets at a rate of 0.1 cells/droplet. This was chosen based on Poisson distribution modelling to limit the number of co-encapsulation events, as previously described (7, 23). Cells were encapsulated in YPD +Kan + 20% Optiprep to achieve neutral buoyancy and select for the ItcR biosensor plasmid (21). *E. coli* biosensors were co-encapsulated with the *Yarrowia* library members at a rate of 10 cells/droplet. Ensuring saturation of biosensor cells within the microdroplet helped minimize fluorescent signal variation due to growth variability of the *E. coli*. Microdroplets were generated using a Sphere Fluidics Fluorescence Activated Droplet Sorter (FADS), in 2.5% Pico-Surf™ in 3M Novec 7500. Oil flowrate was set to 1000uL/hr, and aqueous was set to 800uL/hr to achieve a droplet diameter of roughly 95um. Microdroplets were incubated at 28°C without shaking and with 12-hour oil exchanges to ensure oxygenation of emulsions.

### Emulsion Fluorescence Collection

To achieve biosensor response curves in microdroplets, emulsions of co-encapsulated production strains were run on the FADS (Sphere Fluidics) at a 0 timepoint and 12- or 24-hour intervals to collect histograms of the fluorescence response. No voltage was applied as we were only collecting fluorescent response information. The sorting apparatus was set up as previously described (7). Histograms were exported from the sorting software (Supplementary Figure 1).

### PiggyBac Library Emulsion Sorting

Post-incubation, microdroplets were sorted at four different timepoints, 24, 48, 72 and 96 hours. These timepoints were chosen to represent early (24) mid (48,72) and late (96) fermentation stages. Microdroplets were re-injected into Sphere's Pico-sort chip at a rate between 15-30uL/hr, with spacing oil containing no surfactant (3M Novec 7500) at a rate between 2000-3000 uL/hr to ensure sufficient spacing. Sorting was carried out by applying a voltage to microdroplets as they passed through the sorting chamber as previously described (7). Gating was applied to the top 1% of the population based on fluorescence measurements. 400,000 microdroplets were sorted at each condition to achieve 10X library coverage (with a 0.1 cell/droplet loading frequency). This resulted in the collection of roughly 1000 total sorted isolates. This number varied based on which timepoint was sorted. Specifically, the 24hr timepoint was the most difficult to achieve resolution for and required two iterative rounds of sorting to achieve statistically significant enrichment for improved itaconic acid producers. The second round only collected a total of 800 microdroplets.

### HPLC Analysis

All supernatant samples were filtered with 0.2um nylon filters. Itaconic acid quantification was carried out on an Agilent HPLC, utilizing an Aminex Zorbax aq column with 0.1% TFA in Water as the aqueous phase and 0.1% TFA in Acetonitrile as the organic. All standards for itaconic acid production in *Yarrowia lipolytica* PO1J were made in spent media that matched the composition and time of fermentation of the samples to reduce noise. However, for

complex media (YPD), this increased total background in the spectra and rendered many of our timepoints before the 24-36 hour mark unreliable. Therefore, higher resolution productivity was gathered via fermentation in defined media (YSD) to reduce background.

### Identification of Piggybac Insertion Sites

Thermal asymmetric interlaced (TAIL) PCR was performed as previously described (7). Bands identified from round 3 of the protocol were gel extracted and sent to Eton Bio for sanger sequencing. Sequences received were blasted against the *Yarrowia lipolytica* genome and resulting gene disruptions were identified via KEGG(24). Degenerate primers and nested primers used are in **Table 1** of the supplementary material.

### Confocal Imaging of Droplets

For acquiring images, 10  $\mu$ L of microdroplets were dropped on glass slides and covered with coverslips. The images were collected with a Yokogawa W-1 spinning disk confocal on a Nikon Eclipse-Ti2 inverted microscope (Nikon) equipped with a PLAN APO VC 60x/1.20 water immersion objective. Biosensor emitted fluorescence was excited with a 488nm line from a 50mW Nikon's LUN-F Blues laser and collected with a quadruple bandpass dichroic mirror and a 525/30 emission filter. All images were taken with a Photometrics Prime95B EM-CCD camera controlled with NIS-Elements software. The brightness and contrast of the images captured were adjusted using NIS-Elements software. Image processing was performed using Fiji's ImageJ software.

## Results and Discussion

### Characterization of Biosensor Dynamics in Microdroplets

To elucidate the dynamic range of co-encapsulated biosensors, three established *Yarrowia lipolytica* strains producing TAL (22), Naringenin (20), and Itaconic Acid (19) were co-encapsulated with their corresponding *E. coli* biosensors (7, 21) (**Figure 1a**). Fluorescence measurements were performed on the sorting instrument (Sphere Fluidics) to collect histograms of microdroplet count and fluorescence throughout a 96-hour time course. The top 10% of droplets measured were used to plot a response-curve (**Supplementary Figure 1a-c**). Fluorescence measured at each condition indicate a wide dynamic range from each biosensor (**Supplementary Figure 1**). Interestingly, the itaconic acid strain co-encapsulation with the itaconic acid biosensor shows a longer range with prolonged detection, with increases in fluorescence still occurring past the 84-hour timepoint (**Figure 1b**, **Supplementary Figure 1a**).

Based on these observations, we chose to also obtain confocal images of the microdroplets containing the *Y. lipolytica* itaconic acid production strain and the corresponding *E. coli* biosensor at 24-hour timepoints to provide an additional measurement biosensor fluorescent temporal response and homogeneity (**Figure 1c**). Throughout the time course, these images do suggest some biosensor growth within microdroplets. Therefore, it is possible that in these prolonged sensing conditions net sensor population growth can result in a dilution of analyte response.

However, it is also clear from these images that both the total aggregate fluorescence and biosensor cell-specific fluorescence increases in a dose-responsive/time-dependent manner. Therefore, we chose to use itaconic acid production and sensing as a test case for time course-based sorting of a *Yarrowia lipolytica* piggybac transposon library.

### Timepoint sorting in microdroplets to enrich for itaconic acid overproduction

A library of pathway-engineered *Y. lipolytica* containing piggyBac transposon insertions was used to screen for improved itaconic acid production. To achieve a detectable signal, an *E. coli* biosensor was co-encapsulated with these *Y. lipolytica* strains to achieve fluorescence-dependent readout of concentration. Prior work and efforts described above have demonstrated that *E. coli* and *Y. lipolytica* tolerate one another well in co-culture microdroplets (7), thus enabling both early and late sorting capacity with more accurate timepoints and less emulsion manipulation. Specifically, early timepoint sorting is achievable using co-encapsulation without concern for down-time when using approaches such as pico-injection. Likewise, extended emulsion incubations are enabled without the consequence of disturbing microdroplet stability that can occur during pico-injections due to volume addition and voltage/temperature changes.

Overall microdroplet sorting was carried out as previously described ((7), **Figure 2a**) and isolated the top 1% of fluorescent microdroplets. As previously shown with this itaconic acid producing strain (19), we chose timepoints relevant to previously defined productivity curves and that fell within points of interest in the biosensor response curves from microdroplets. In this experiment, the library sorting was conducted at four distinct timepoints (24, 48, 72, and 96 hours) to determine the impact of sorting time on productivity and final titer. Populations of sorted isolates were characterized through analysis of 24 colonies from each timepoint, along with their corresponding unsorted controls. The unsorted control was obtained via the same sorting method (including applied voltage), but with no gate applied followed by a similar plating and selection workflow. These isolated strains were cultivated at the test-tube scale and supernatant samples were analyzed for itaconic acid quantification via liquid chromatography (Agilent Zorbax aq). In each of these cases, enriching the piggyBac library for improved itaconic acid production resulted in successful, statistically significant (Welch's correction T-test) separation of populations at most timepoints compared with a control, unsorted pool isolated at that same timepoint (**Figure 2b**). However, due to the nature of the 24-hour biosensor response, and the need to iteratively sort this population, this sorted population versus the unsorted control did not show significant differences, likely due to the previously characterized response curve. However, since much of the sorted population still produced more than the unsorted, the population was still characterized to determine enrichment capabilities as this timepoint. Successful population enrichment from these sorts at all timepoints indicates that the dynamic range, sensitivity, and saturation properties of the biosensor was sufficient to achieve signal differentiation at each timepoint.

### Flask-based time course experiments highlight parallels with sorting

After confirming successful sorts of each timepoint, all isolates demonstrating an itaconic acid production level above the mean from the respective sorted condition were selected for a flask-scale time course experiment. To do so, each isolate was grown in 250mL flasks containing 50mL YPD media with 2% glucose at 28 °C with timepoints taken every 12 hours for a total of 96 hours. Collective production curves for each of the populations show clear trends with respect to production capability (**Supplementary Figure 3**). d

To further compare productivity trends, itaconic acid production from the flask time course is segmented and represented as a percent of total production at Early (48-36), Mid (72-48) and Late (96-72) timepoints in the flask (**Figure 3ai-iv**). For strains that were isolated using early sort timepoints (24 and 48 hours in microdroplets), most of the productivity in the flask was likewise biased toward early timepoints (in this case, 36-48 hours) with strains peaking in production at around 60 hours (**Figure 3ai-ii**). For strains isolated at the late timepoints (72 and 96 hours), productivity was more gradual in the culture with more itaconic acid produced late in the culture, especially at the 72-96 hour flask timepoints (**Figure 3aiii-iv**). It is worth noting that these late-sorting cells ultimately peak at a slightly higher final titer (**Supplementary Figure 3b**). Most striking, however, is the clear difference in percent production profile between the strains isolated at 24- and 96-hour sorts (**Figures 3ai, 3aiv**).

To determine if these phenotypes were linked to cell growth/biomass accumulation, itaconic acid titer was normalized to OD for the 24 and 96-hour sort condition strains (**Figure 3b**). The production patterns obtained here are fairly like the non-normalized curves (**Supplementary Figure 2a-b**) and once again highlight a higher productivity earlier in the fermentation for cells isolated in the 24-hour sort compared with the 96-hour sort. The normalized total production is also still higher for the strains isolated from the 96-hour sort. As a result, different productivity profiles and capacities are identified when distinct microdroplet selection conditions are imposed.

Due to the high overlap of response curves in each condition that shared phenotypic production, the top 5 characterized isolates from each condition Top (**Figure 2b**) at each of the timepoints were preserved and isolated genomic DNA was used as a template in TAIL PCR (7, 25-28) for transposon insertion site identification. It is interesting to note that the various selection conditions gave rise to both unique production phenotypes and distinct genetic targets. Specifically, an insertion in the *Ypmg1* gene responsible for phosphorylation in the glycolysis pathway was predominately isolated from the 24 and 48-hour best performing isolates. In contrast, the 72- and 96-hour best isolates both converged on the same insertion in the *Ygsy1* gene which controls glycogen storage. Disruption location identification was carried out via sequencing analysis and alignment utilizing KEGG (24). Sequencing results can be found in the supplementary information appendix. Interestingly, the 24-hour sort appears to exhibit a range of production phenotypes, the very late-stage production phenotype as well as the early-stage productivity (**Supplementary Figure 3a**). It is thus not overly surprising that some lower-performing isolates from the 24-hour sort, but not the 48, show the same, *Ygsy1*, gene perturbation as the later sorts. Target convergence within each sort indicates the robustness of the screening system, and the 24-hour

dual-phenotype isolation may also indicate the timepoint at which these phenotypes diverge to be isolated individually.

Both genotypes identified contain disruptions in glycogen synthesis and storage. Due to itaconic acid production utilizing TCA cycle intermediates, these disruptions likely lead to higher flux through glycolysis, rather than glycogen synthesis, thus resulting in more carbon source available to divert to itaconic acid production. The difference in perturbation for early versus late producers indicates the role these genes play in cell mass accumulation at different stages of cell growth. Previous studies utilizing microfluidic screening for small molecule production typically utilize previously-defined bioreactor or flask-relevant time points. Thus, we chose to analyse more than just the end-point to determine if other phenotypes could be pulled that would be relevant to scaled-up production.

Interestingly, both of the piggybac insertions identified here for itaconic acid production have also been identified for the production of Naringenin and TAL in *Yarrowia lipolytica* (7). These previous screens also utilized a similar biosensor-in-microdroplet approach to identify improved production of these small molecules. Re-identification of these gene targets increases the likelihood that their disruption could be beneficial for many small molecule production applications in this yeast.

#### Characterizing the in-microdroplet conditions for top performers to understand strain-biosensor dynamics

To better characterize the correspondence between flask and microdroplet scale, we re-encapsulated representative isolates from each of the major populations described above into *Y. lipolytica* mono-culture emulsions along with the *E. coli* biosensor. These mono-culture emulsions were incubated for a total of 96 hours once again and run on the FADS (Sphere Fluidics) at 24, 48, 72 and 96 hours (**Supplementary Figure 4, Figure 3c**). Fluorescent measurements for isolates at each production stage were collected via the microdroplet sorting system, allowing for a direct comparison between fluorescence obtained and sorted in initial experiments to their best-performing timepoints. Overlay of fluorescent response in droplets to production in flasks for the 24hr and 96hr best isolates show significant overlap (**Figure 3c**). Patterns show similar responses to those seen in the initial wildtype experiment (**Figure 1b**), with the biosensor fluorescence increasing greatly at the final, 96-hour timepoint. However, this is likely due to accumulation of product over time, and interestingly, the biggest differences between isolates can be seen in the fold-change of fluorescence between the earliest timepoint (24 hours), and the final timepoint (96 hour). In particular, the 24-hour isolate showed a 2-fold increase in fluorescence between the 24-hour timepoint and 96-hour whereas the 96-hour isolate shows an increase of almost 5-fold in fluorescence. This difference corresponds well with the production profiles that indicate an early plateau for the earliest-selected isolates (**Figure 3a, Supplementary Figure 2**).

## Conclusions

Microdroplet sorting using cell-based biosensors has expedited the Design-Build-Test cycle for metabolic engineering and synthetic biology, especially for the case study of improved small molecular

production (7, 9, 10, 18). By characterizing three distinct biosensor dynamics in microdroplets, we identified extended dose-response ranges to production. In particular, we recognized an opportunity to utilize an itaconic acid biosensor, with its increased response range in microdroplets, for production phenotype sorting. Utilizing this, we were able to showcase the flexibility of a microdroplet environment to uniquely allow for selections of strain productivity for itaconic acid producing *Yarrowia lipolytica*. This allowed us to connect in-microdroplet production to in-flask production and recapitulate those phenotypes from microdroplets to flasks.

Through this experiment, we showcased distinct early versus late production phenotypes obtained from time course-based sorting and identified two insertions responsible for these different production changes. Applications of this time course-based system could be used to tailor high throughput screening for limited biosensor dynamic ranges, improving strain productivity, or identifying ideal sorting times for improving production using gene perturbation libraries.

## Author Contributions

E.K.B, H.A., P.T.N.H. designed experiments. E.K.B, A.R.G.S, conducted biosensor-in-droplet data collection. A.R.G.S., K.M.V.N. performed confocal imaging. E.K.B., P.T.N.H, performed library sorting. E.K.B. conducted data analysis. E.K.B, H.A., wrote the manuscript.

## Conflicts of interest

There are no conflicts to declare.

## Acknowledgements

This work was in part by the Air Force Office of Scientific Research under Award No. FA9550-14-1-0089. This work was also funded in part by São Paulo Research Foundation – FAPESP, Brazil (Grant number 2021/13808-2). Confocal imaging was performed at the Center for Biomedical Research Support Microscopy and Imaging Facility at UT Austin (RRID# SCR\_021756). The Sphere Fluidics system was funded by a Cooperative Agreement (W911NF-17-2-0091) between Army Research Laboratory (ARL) and UT Austin. Opinions, conclusions, interpretations, and recommendations are those of the authors and are not necessarily endorsed by the US Army. The mention of trade names or commercial products does not constitute endorsement or recommendation for use by the Department of the Army or the Department of Defense.

## Figure Legends:

**Figure 1: Biosensor dynamics in microdroplets.** a) Workflow of emulsion generation and data collection for fluorescence at selected timepoints. Top performing isolates or wildtype were encapsulated with the same method as sorted isolates. Created with BioRender.com. Created with BioRender.com. b) Biosensor response dynamics in droplets were measured over time. The itaconic acid producing parental strain of *Y. lipolytica* was encapsulated with the corresponding *E. coli* biosensor and fluorescence was measured on the microdroplet sorter in 12-hour increments. c) Parental strain fluorescence changes within microdroplets were captured with Nikon™ spinning disk confocal imaging. These measurements are normalized to the total area measured for fluorescence. To characterize the itaconic acid biosensor response in droplets more clearly, emulsions were imaged on a spinning disk confocal and fluorescence intensity at each timepoint was measured (with representative images shown on the right).

**Figure 2: Time course sorting of *Y. lipolytica* piggybac library for itaconic acid production.** a) A Piggybac transposon library was generated in an itaconic acid-producing strain of *Y. lipolytica* (19, 29) and co-encapsulated with the itaconic acid *E. coli* biosensor at a ratio of **1 producer cell to every 10 droplets, and 10 *E. coli* biosensor cells to every droplet, or 0.1:10 *Y. lipolytica*:*E. coli***. After timed incubation of either 24, 48, 72 or 96 hours, emulsions were then sorted using the GFP signal. Created with BioRender.com. b) Post-sort, emulsions were broken and cultivated in a mixed population and plated for single colonies on YPD-agar plates. US = unsorted, S = sorted. Unsorted is the same emulsion isolated at the same timepoint but with no selection gate applied, sorted is the same emulsion with a selection gate for the top 2% of cell-containing droplets. Random isolates from the sort and an unsorted control were picked from plates and grown in YPD on the tube-scale for their respective fermentation time that corresponded with the sorting timepoint. Supernatant was isolated and itaconic acid titer quantified via HPLC to determine if the sorts were successful.

**Figure 3: Time course fermentations for production phenotype characterization.** Top 24 isolates identified from each sort were cultured in flasks for a total of 96 hours with itaconic acid production and OD sampled every 12 hours. a) Percent production of itaconic acid at early (36-48hr) mid (72-48) and late (96-72) timepoints for 24 (i), 48 (ii), 72hr (iii) and 96 (iv) hour sorts. Isolates chosen for evaluation represent the top 24 identified from initial sort analysis (Figure 2b). Percent production at each segment of fermentation was calculated as the change in itaconic acid titer between the timepoints divided by the total final titer. b) Biological triplicate of defined media fermentations of top performing isolate from 24 and 96 hour timepoints show the same patterns of production as the rich media. In addition, significant production doesn't seem to begin until the 48-hour timepoint for both conditions. This indicates that rich media fermentations, while plagued by high background, still show a clear picture of what production looks like in a flask for these strains. c) The top performing isolate from each sorting condition was re-encapsulated with biosensor and fluorescence was collected via the droplet sorter. Fluorescence for each isolate was collected on separate days, therefore only comparisons can be made within each isolate, not between.

## References

1. Y. Liu, J. Nielsen, Recent trends in metabolic engineering of microbial chemical factories. *Curr Opin Biotechnol* **60**, 188-197 (2019).
2. E. K. Bowman, H. S. Alper, Microdroplet-Assisted Screening of Biomolecule Production for Metabolic Engineering Applications. *Trends Biotechnol* **38**, 701-714 (2020).
3. M. T. Guo, A. Rotem, J. A. Heyman, D. A. Weitz, Droplet microfluidics for high-throughput biological assays. *Lab Chip* **12**, 2146-2155 (2012).
4. J. L. Lin, J. M. Wagner, H. S. Alper, Enabling tools for high-throughput detection of metabolites: Metabolic engineering and directed evolution applications. *Biotechnol Adv* **35**, 950-970 (2017).
5. M. Rienzo *et al.*, High-throughput screening for high-efficiency small-molecule biosynthesis. *Metab Eng* **63**, 102-125 (2021).
6. M. Rothbauer, H. Zirath, P. Ertl, Recent advances in microfluidic technologies for cell-to-cell interaction studies. *Lab Chip* **18**, 249-270 (2018).
7. E. K. Bowman *et al.*, Sorting for secreted molecule production using a biosensor-in-microdroplet approach. *Proc Natl Acad Sci U S A* **118** (2021).
8. D. Li, L. Liu, Z. Qin, S. Yu, J. Zhou, Combined evolutionary and metabolic engineering improve 2-keto-L-gulonic acid production in *Gluconobacter oxydans* WSH-004. *Bioresour Technol* **354**, 127107 (2022).
9. X.-D. Zhu *et al.*, High-throughput screening of high lactic acid-producing *Bacillus coagulans* by droplet microfluidic based flow cytometry with fluorescence activated cell sorting. *RSC Advances* **9**, 4507-4513 (2019).
10. T. E. Saleski *et al.*, Syntrophic co-culture amplification of production phenotype for high-throughput screening of microbial strain libraries. *Metab Eng* **54**, 232-243 (2019).
11. D. Xiong *et al.*, Improving key enzyme activity in phenylpropanoid pathway with a designed biosensor. *Metab Eng* **40**, 115-123 (2017).
12. W. W. Liu, Y. Zhu, Q. Fang, Femtomole-Scale High-Throughput Screening of Protein Ligands with Droplet-Based Thermal Shift Assay. *Anal Chem* **89**, 6678-6685 (2017).
13. D. A. Holland-Moritz *et al.*, Mass Activated Droplet Sorting (MADS) Enables High-Throughput Screening of Enzymatic Reactions at Nanoliter Scale. *Angew Chem Int Ed Engl* **59**, 4470-4477 (2020).
14. S. M. Bjork, S. L. Sjostrom, H. Andersson-Svahn, H. N. Joensson, Metabolite profiling of microfluidic cell culture conditions for droplet based screening. *Biomicrofluidics* **9**, 044128 (2015).
15. L. Boitard *et al.*, Monitoring single-cell bioenergetics via the coarsening of emulsion droplets. *Proc Natl Acad Sci U S A* **109**, 7181-7186 (2012).
16. R. J. van Tatenhove-Pel *et al.*, Serial propagation in water-in-oil emulsions selects for *Saccharomyces cerevisiae* strains with a reduced cell size or an increased biomass yield on glucose. *Metab Eng* **64**, 1-14 (2021).
17. H. Bachmann, J. T. Pronk, M. Kleerebezem, B. Teusink, Evolutionary engineering to enhance starter culture performance in food fermentations. *Curr Opin Biotechnol* **32**, 1-7 (2015).
18. B. L. Wang *et al.*, Microfluidic high-throughput culturing of single cells for selection based on extracellular metabolite production or consumption. *Nat Biotechnol* **32**, 473-478 (2014).
19. J. Blazeck *et al.*, Metabolic engineering of *Yarrowia lipolytica* for itaconic acid production. *Metab Eng* **32**, 66-73 (2015).
20. C. M. Palmer, K. K. Miller, A. Nguyen, H. S. Alper, Engineering 4-coumaroyl-CoA derived polyketide production in *Yarrowia lipolytica* through a  $\beta$ -oxidation mediated strategy. *Metab Eng* **57**, 174-181 (2020).
21. E. K. R. Hanko, N. P. Minton, N. Malys, A Transcription Factor-Based Biosensor for Detection of Itaconic Acid. *ACS Synth Biol* **7**, 1436-1446 (2018).
22. K. A. Markham *et al.*, Rewiring *Yarrowia lipolytica* toward triacetic acid lactone for materials generation. *Proc Natl Acad Sci U S A* **115**, 2096-2101 (2018).
23. L. Mazutis *et al.*, Single-cell analysis and sorting using droplet-based microfluidics. *Nat Protoc* **8**, 870-891 (2013).
24. M. Kanehisa, Y. Sato, M. Kawashima, M. Furumichi, M. Tanabe, KEGG as a reference resource for gene and protein annotation. *Nucleic Acids Res* **44**, D457-462 (2016).
25. Y.-G. Liu, R. F. Whittier, Thermal asymmetric interlaced PCR: automatable amplification and sequencing of insert end fragments from P1 and YAC clones for chromosome walking. *Genomics* **25**, 674-681 (1995).
26. D. Liu *et al.*, Construction, Model-Based Analysis, and Characterization of a Promoter Library for Fine-Tuned Gene Expression in *Bacillus subtilis*. *ACS Synth Biol* **7**, 1785-1797 (2018).
27. J. Fonager *et al.*, Development of the piggyBac transposable system for *Plasmodium berghei* and its application for random mutagenesis in malaria parasites. *BMC Genomics* **12**, 155 (2011).
28. D. Kalyani *et al.*, A Highly Efficient Recombinant Laccase from the Yeast *Yarrowia lipolytica* and Its Application in the Hydrolysis of Biomass. *PLOS ONE* **10**, e0120156 (2015).
29. J. M. Wagner, E. V. Williams, H. S. Alper, Developing a piggyBac Transposon System and Compatible Selection Markers for Insertional Mutagenesis and Genome Engineering in *Yarrowia lipolytica*. *Biotechnol J* **13**, e1800022 (2018).



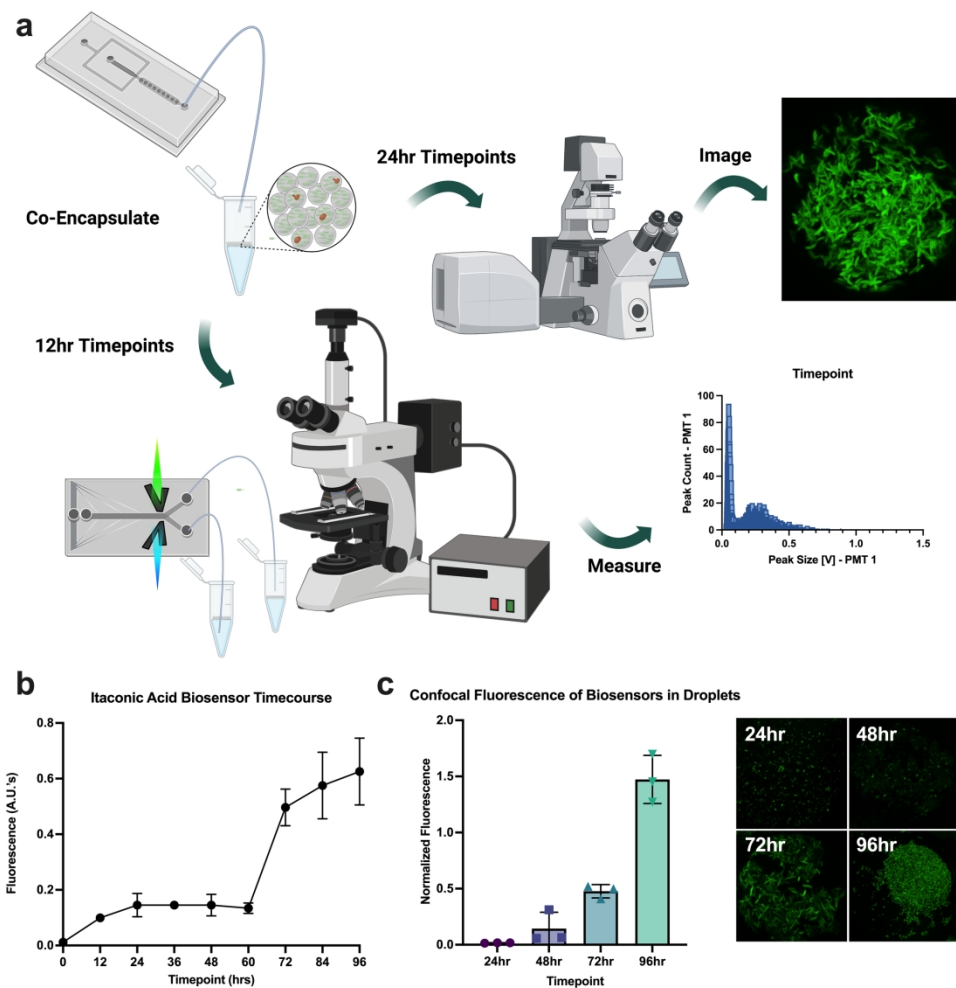


Figure 1

215x217mm (300 x 300 DPI)

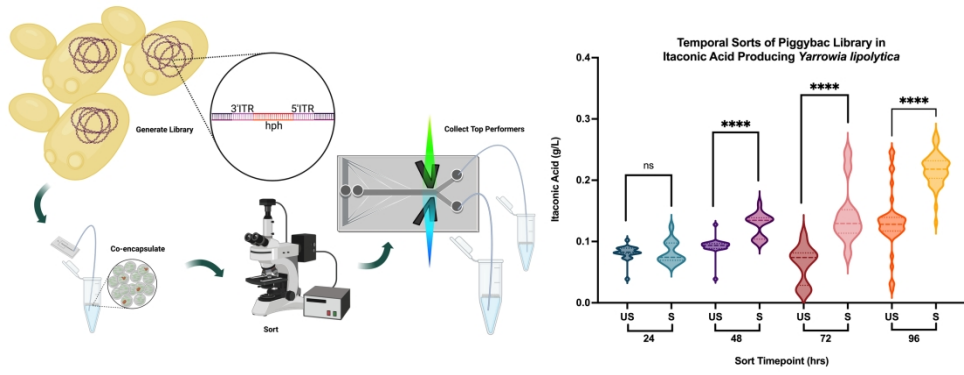


Figure 2

280x109mm (300 x 300 DPI)

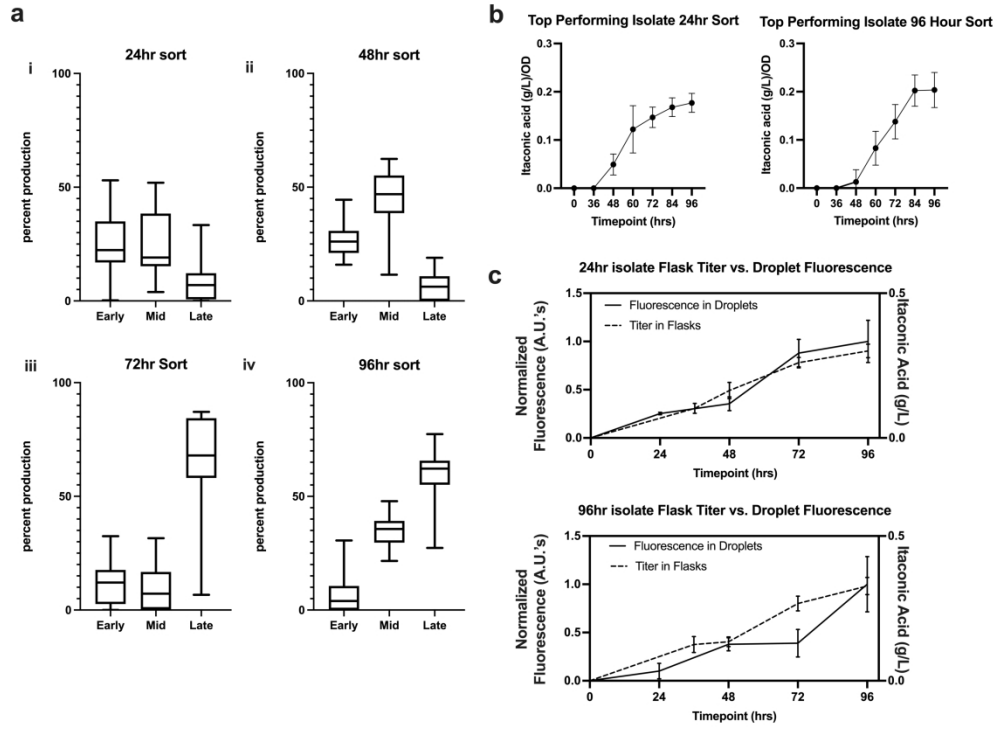


Figure 3

276x204mm (300 x 300 DPI)